Photochemical ozone pollution in the Valparaiso Region, Chile

**Richard A. Toro · Camila S. Donoso · Rodrigo A. Seguel ·
Raúl G. E. S. Morales · Manuel A. G. Leiva**

Abstract The Valparaiso Region is characterized by the presence of air sheds that modulate the general atmospheric circulation with local winds. The ozone concentration in the region increases from the west coast toward the mountainous area, where the concentrations of ozone precursors are lower. In this study, surface ozone (O_3), nitric oxide, nitrogen dioxide, nitrogen oxide (NO_x), and volatile organic compounds (VOCs) were measured at four sites, including two upwind urban sites (Viña del Mar (VM) and Villa Alemana (VA)), an upwind suburban site (Quillota (QU)) and a downwind semirural site (Los Andes (LA)) during 01 March–07 April 2010. The purpose of this study is to improve our understanding of the photochemistry of ozone in urban and semirural areas of the Valparaiso Region and the transport of ozone pollution in downwind rural areas. The results show that, in the VM and VA sites, higher concentrations of ozone precursors, NO_x, and VOCs, are observed in the early morning hours, which is related to emissions from vehicle traffic, while comparatively lower ozone precursor concentrations are observed in QU and LA. In contrast, higher ozone concentrations are found in LA and QU, and lower concentrations are found in VM and VA. VOC analysis was performed by gas chromatography, and the results show that the VOC composition in the studied sites is similar to and coincident with vehicle emissions. An ozone formation regime limited by VOCs is found in the area. The leading contributors to the ozone-forming potential were ethene, propene, xylene, and toluene, which are also anthropogenic species and account for more than 70 % of O_3 formation. Thus, benzenes–toluene–xylenes played the most important role in O_3 formation, followed by alkenes, alkanes, aromatic, biogenic, and alkynes during the study periods. The m-, p-xylene/ethylbenzene relation confirms the reception of aged air masses in LA. The results of the present study demonstrate that ozone pollution is a regional problem and that O_3 regional transport is associated with such pollution. Finally, the results indicate the need to adopt mitigating measures for ozone pollution that consider the reactivity characteristics of VOCs.

Keywords Pollution—urban and regional · Tropospheric ozone · Non-methane hydrocarbons · Ozone formation potential

R. A. Toro · C. S. Donoso · R. G. E. S. Morales ·
M. A. G. Leiva (✉)
Centro de Ciencias Ambientales and Departamento de Química,
Facultad de Ciencias, Universidad de Chile, Casilla 653
Santiago, Chile
e-mail: manleiva@uchile.cl

M. A. G. Leiva
e-mail: manleiva@me.com

R. A. Seguel
Centro Nacional del Medio Ambiente, Universidad de Chile,
Avenida Larraín 9975, La Reina, Santiago, Chile

R. A. Seguel
Department of Atmospheric and Oceanic Sciences, University of
California, Los Angeles, CA, USA

M. A. G. Leiva
Department of Land, Air and Water Resources, University of
California, Davis, CA, USA

Introduction

Since the middle of the 1950s, many studies have established that the formation of ozone (O_3) in the troposphere is promoted by the presence of volatile organic compounds (VOCs) (Fenger 2009). VOCs participate in atmospheric chemistry through radical oxidation reactions (Denisov 2008). Generally, for most VOCs, oxidation is initiated by reaction with hydroxyl radicals (OH). The final result is the formation of ozone and nitrogen dioxide (available for the formation of more ozone), the regeneration of the OH radical (available to

catalyze ozone formation), and various other chemical species (Jacob 1999; Morales 2006; Seinfeld and Pandis 2012). Some VOCs form intermediate compounds that act as temporary reservoirs and can form less volatile compounds capable of participating in the formation of secondary organic aerosols (SOA) (Camredon et al. 2007).

The efficiency of the ozone formation process is determined by the relationship between the nitrogen oxides (NO_x) and VOCs (Pusede and Cohen 2012; Vivanco 2008), while the formation rate of ozone is mainly controlled by the rate of the initial reaction of VOCs with OH radicals. Next, the contribution of each VOC to the formation of ozone becomes a function of its reactivity (Avery 2006; Pusede and Cohen 2012; Seguel et al. 2013). In this way, knowing the sources, concentrations, and chemical reactivity of VOCs in relation to the formation of O_3 and SOA is essential for the development of photochemical pollution control strategies in areas impacted by ozone, such as the Valparaíso Region (VR) in Chile (see Fig. 1).

The VR is located in the central area of Chile and is characterized by the presence of air sheds that modulate the general atmospheric circulation with local winds, sea–land breezes at coast locations, and valley breezes at the mountain locations (DMG 2013). It is the third most inhabited region of the country and is where the most important port of the country is located (IGM 2013; INE 2013). As a consequence

of development, the urban areas of this region have experienced decreased air quality in recent years. However, information regarding the atmospheric concentrations of ozone and its precursors is limited and/or non-existent (MMA 2011; SINCA 2013).

In the present work, we discuss the results of the measurement of various ozone precursors (NO_x and 71 VOCs) in the summer period between March and April 2010 at four sites of the VR, located from the southwest toward the northwest of the region (SW-NE). First, the composition and reactivity of each ambient VOC mixture is characterized in regard to its ambient concentration and its ozone forming potential; second, the transport of air masses from the upwind areas to the downwind areas is evaluated. Finally, the results allow us to extend our knowledge of the photochemical processes involved in the formation of ozone in the atmosphere of VR and to evaluate the ozone formation regime to establish and improve the control measures of ozone pollution in the study area.

Experimental methods

Study area

The study area corresponds to the VR, which extends between 32°02′ and 33°58′ of S latitude (IGM 2013), as can be seen in
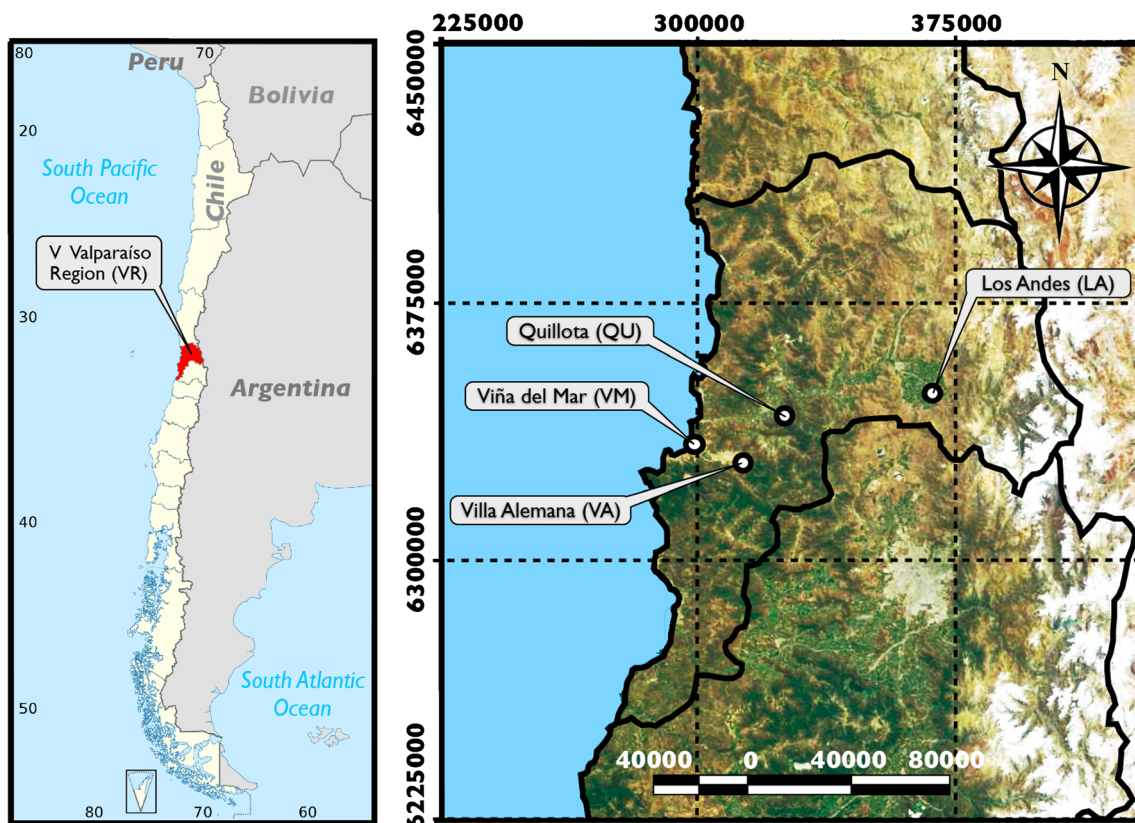

Fig. 1 The sampling sites of Valparaíso Region (*VR*) in Chile

Fig. 1. Historically, this region has been the most important port area of Chile and the third most populous area of the country, with a population of 1,723,547 inhabitants in the year 2012, corresponding to 10.4 % of the country's total population (INE 2013). The region has a surface area of 16,396 km^2 and offers a significant percentage of the economic productivity of the country (IGM 2013). Its main cities are the Viña del Mar-Valparaiso co-urbanization, Quillota, Villa Alemana, and Los Andes. The VR presents Mediterranean weather (DMG 2013), characterized by a rainy winter period and a dry summer period. Mild temperatures are maintained at the coast with humidity in the air, materializing as low clouds and a sea breeze. Additionally, the inland is characterized as presenting more elevated temperatures and lower relative humidity (DMG 2013).

A description of the sampling sites and schedule

Four sampling sites were selected (see Table 1 and Fig. 1), located in the urban centers of Viña del Mar (VM), Villa Alemana (VA), Quillota (QU), and Los Andes (LA). The selected sites allow evaluations of the possible impact of the locally produced emissions as well as their transport toward the interior of the airshed, in the case of the LA station.

According to their surrounding environments and locations, the monitoring stations can be described as follows: VM is located in the central coast, next to the mouth of the Estero Marga-Marga to the Pacific ocean, and is an urban area, which is impacted by the Valparaiso port activity and the surrounding industrial parks; VA is located in an urban area oriented toward services, and it is 16 km from VM; QU is a semi-urban area with agricultural and mining activities, is characterized by the presence of thermoelectric plants, and is located 35 km from VM; LA is located in the transitional area between the Aconcagua valley and the foothills of the Andes Mountain Range, is an urban area with agriculture and mining as the main activities, and is located 92 km from VM.

Sampling and monitoring

At each site, the monitoring of the ambient O_3 concentration, NO_x, and meteorological variables, i.e., wind speed and wind direction, relative humidity, and temperature, was performed with continuous measurement equipment (see Table 1). The measurements of the O_3 and NO_x ambient concentrations were performed using the 49i/Thermo Environmental Monitor and 42i/Thermo Environmental monitoring equipment (Thermo Fisher Scientific Inc., Waltham, MA, USA), respectively. The data were validated to identify gaps, duplicated data, and/or anomalous data. For the VOCs, discrete samplings were performed on week days and weekends for 4-h periods during the morning (0600 to 1000 hours) and in the afternoon (1200 to 1600 hours). These periods are characterized by anthropogenic emissions during the morning and high photochemical activity in the afternoon. Measurements during the evening/night time were also performed at some sites (1800 to 2200 hours). The measurement campaigns of ambient VOC concentrations were performed simultaneously in the four sampling sites.

The speciation of VOCs was performed with individual stainless steel containers (canisters), each with a 6-l capacity and a SUMMA® inner lining. The procedure is based on the pressurized sampling method described in the USEPA A-14A Method (US-EPA 1999a).

Analysis of volatile organic compounds

The canister samples were analyzed at the Desert Research Institute, Reno, NV, USA. Seventy-one VOCs were measured (see Table 2) using a gas chromatography/mass spectrometry technique, according to the EPA Method TO-15 (US-EPA 1999b). The gas chromatography–flame ionization detector–mass spectrometry (GC-FID/MS) system included a Lotus Consulting Ultra-Trace Toxics sample pre-concentration system built into a Varian 3800 gas chromatograph with a flame

Table 1 The locations of the sampling sites and the sampling period

| | Sampling stations | | | |
	Viña del Mar	Villa Alemana	Quillota	Los Andes
Site Code	VM	VA	QU	LA
Latitude (S)	33°01′13″	33°03′19″	32°53′27″	32°50′45″
Longitude (W)	71°33′00″	71°23′27″	71°12′35″	70°35′12″
Altitude (masl)	19	144	138	839
O_3 and NOx Sampling period (MM/DD/YY to MM/DD/YY)	16 March to 6 April 2010	16 March to 7 April 2010	1 March to 7 April 2010	1 March to 6 April 2010
VOCs sampling period (MM/DD/YY)	17, 18, 21, 24, 25 March 2010	17, 18, 21, 24, 25 March 2010	24, 25 March 2010	17, 18, 21, 24, 25 March 2010

Table 2 A list of the VOCs under study, their classification based on their chemical nature, and maximum incremental reactivity scale (MIR, listed in Carter and Heo 2012) of the individual VOCs

No. ID	Compounds	Family	MIR	No. ID	Compounds	Family	MIR	No. ID	Compounds	Family	MIR	No. ID	Compounds	Family	MIR
1	Acetylene	ALY	0.93	19	trans-2-Pentene	ALE	10.25	37	2,3-Dimethylpentane	ALA	1.26	55	o-Xylene	BTXs	7.44
2	Ethene	ALE	8.76	20	cis-2-Pentene	ALE	10.07	38	Cyclohexene	ALE	4.81	56	n-Nonane	ALA	0.71
3	Ethane	ALA	0.26	21	2-Methyl-2-Butene	ALE	13.72	39	3-Methylhexane	ALA	1.51	57	Isopropylbenzene	ARO	2.43
4	Propene	ALE	11.37	22	2,2-Dimethylbutane	ALA	1.11	40	cis-1,3-Dimethylcyclopentane	ALA	1.82	58	n-Propylbenzene	ARO	1.95
5	Propane	ALA	0.46	23	Cyclopentene	ALE	6.55	41	1-Heptene	ALE	4.25	59	alpha-pinene	BIO	4.38
6	1,3-Butadiene	ALE	12.21	24	Cyclopentane	ALA	2.25	42	2,2,4-Trimethylpentane	ALA	1.20	60	3-Ethyltoluene	ARO	7.21
7	1-Butene	ALE	9.42	25	2,3-Dimethylbutane	ALA	0.91	43	n-Heptane	ALA	0.99	61	4-Ethyltoluene	ARO	4.32
8	cis-2-Butene	ALE	13.89	26	2-Methylpentane	ALA	1.41	44	2,3-Dimethyl-2-Pentene	ALE	9.45	62	1,3,5-Trimethylbenzene	ARO	11.44
9	Isobutylene	ALE	6.14	27	3-Methylpentane	ALA	1.70	45	Methylcyclohexane	ALA	1.58	63	o-Ethyltoluene	ARO	5.43
10	trans-2-Butene	ALE	14.79	28	2-Methyl-1-Pentene	ALE	5.12	46	2,3,4-Trimetilpentano	ALA	0.96	64	1,2,4-rimethylbenzene	ARO	8.64
11	n-Butane	ALA	1.08	29	n-Hexane	ALA	1.15	47	Toluene	BTXs	3.88	65	n-Decane	ALA	0.62
12	Isobutane	ALA	1.17	30	trans-2-Hexene	ALE	8.37	48	2-Methylheptane	ALA	0.99	66	1,2,3-Trimethylbenzene	ARO	11.66
13	1,2-Butadiene	ALA	1.36	31	cis-2-Hexene	ALE	8.06	49	4-Methylheptane	ALA	1.16	67	Indane	ARO	3.20
14	Isopentane	ALA	1.23	32	trans-1,3-Hexadiene	ALE	10.03	50	3-Methylheptane	ALA	1.15	68	1,3-Diethylbenzene	ARO	6.92
15	1-Pentene	ALE	9.03	33	Methylcyclopentane	ALA	2.06	51	n-Octane	ALA	0.82	69	1,4-Diethylbenzene	ARO	4.31
16	2-Methyl-1-Butene	ALE	6.97	34	2,4-Dimethylpentane	ALA	1.46	52	Ethylbenzene	ARO	2.93	70	n-Butylbenzene	ARO	2.27
17	n-Pentane	ALE	6.23	35	Bencene	BTXs	0.69	53	m-, p-Xylene	BTXs	7.61	71	n-Undecane	ALA	0.55
18	Isopropene	BIO	10.28	36	2-Methylhexane	ALA	1.10	54	Styrene	ARO	1.65				

ionization detector, which was coupled to a Varian Saturn 2000 ion trap mass spectrometer (Agilent Technologies, Santa Clara, CA, USA). Light hydrocarbons were deposited onto a Varian CP-Sil5 column (15 m×0.32 μm×1 μm), which was plumbed to a column-switching valve in the GC oven, and then to a Chrompack Al_2O_3/KCl column (25 m× 0.53 mm×10 μm), which led to the FID for quantitation of the light hydrocarbons (C2–C4). The midrange and heavier hydrocarbons were cryo-focused in the rear trap and deposited onto a J&W DB-1 column (60 m×0.32 mm×1 μm) that was connected to the ion trap mass spectrometer. The initial GC temperature was 5 °C, which was held for approximately 9.5 min before ramping at 3 °C/min to 200 °C for a total run time of 80 min.

System calibration was conducted using a mixture that contained the most commonly found hydrocarbons in the range of 0.2 to 10 ppb. Three-point external calibrations were run prior to analysis, and one calibration check was run every 24 h. Replicate analyses were conducted at least 24 h after the initial analysis to allow re-equilibration of the compounds within the canister.

All detection limits are in the range of 0.01–0.05 ppbv (depending on VOC) and precision is less than 10 %. All samples are corrected for lot-specific sampling media blank values prior to the final concentration calculations.

Results and discussion

The variation of O_3 and its precursors (NO_x and VOCs)

Figure 2 shows the time series of the variation of ozone, NO_x, and total VOC concentration (TVOC) in the four sites under study in the VR. It is also possible to characterize two periods of higher ozone concentration in the sampling campaigns: the first between days 17 and 21 of March 2010, and the second between days 23 and 26 of March 2010. Generally, the daily pattern shows the existence of two maxima for NO_x during the day: one appears during the morning between approximately 0700 and 0900 hours, and the other appears during the after-noon after 1800 hours, which is most likely associated with the hours of higher vehicle transit (Sawyer 2010; Seguel et al. 2012, 2013). This pattern is similar to that observed for the TVOC case, in which the lower concentrations appear around noon and the higher concentrations appear during the morning and the evening. In contrast, O_3 has only one maximum at noon, which is related to the daily solar radiation cycle and is due to the ozone photochemical nature (Seinfeld and Pandis 2012). The maximum ozone concentration is observed at 1300–1400 hours in the VM and VA sites, but it was delayed by at least 1 h between 1400 and 1500 hours in the suburban and rural sites (i.e., QU and LA). The delay in the ozone peaks is indicative of the possible regional transport of ozone air
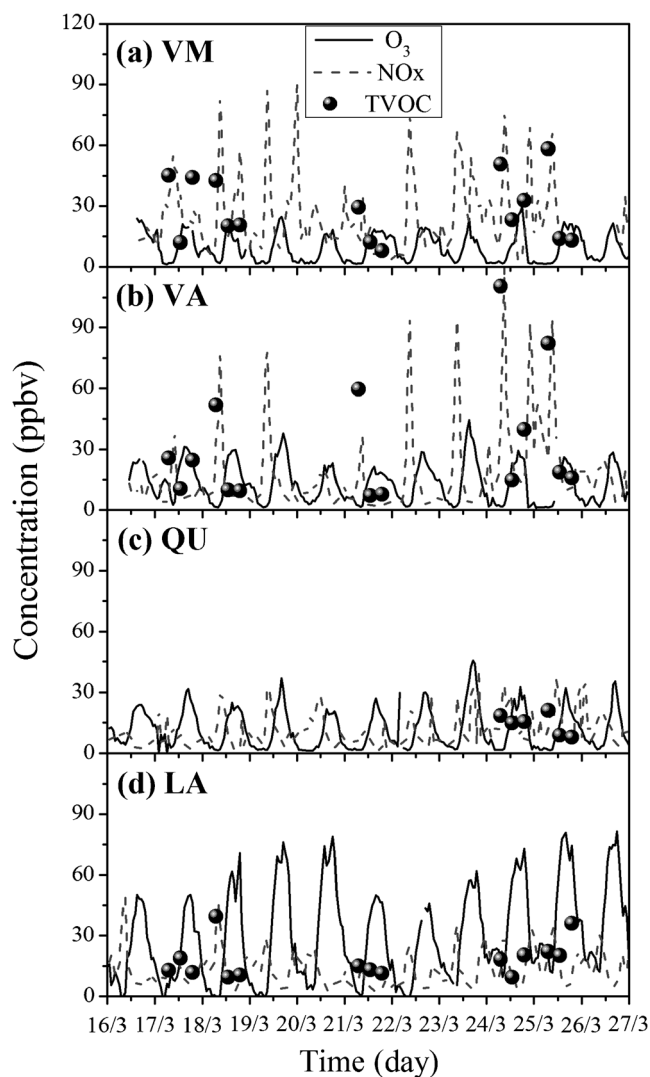

Fig. 2 The time series of the variation of ozone, NOx, and total VOC concentration (TVOC) in the four sites under study in the VR

masses and their precursors from urban areas, located at the coast, toward the semi-urban areas located near the interior of the region (Adame and Sole 2013; Zhang and Ying 2011).

Table 3 shows a statistical summary of the average hourly mixing ratios of O_3 and its precursors, NO, NO_2, NO_x, and TVOC. The data indicate that there is a concentration gradient of the different sampling sites. Generally, the concentrations of NO, NO_2, and NO_x are higher in the urban areas located at the coast (VM and VA) and lower in the semi-urban areas located toward the interior of the region (QU and LA). The 1-h average concentrations of NO in VM, VA, and QU are 6.7, 3.8, and 1.7 times higher than that observed in LA (2.29± 4.12 ppbv). For the 1-h average concentrations of NO_2, the values are 0.6 to 0.8 times than that observed in LA (12.2± 6.85 ppbv) for the other stations. No significant variations are observed between the ambient concentrations for the different sampling sites of NO_2. In the case of the 1-h average of NO_x (NO_x=NO+NO_2) concentrations, the values are 1.8, 1.2, and

Table 3 The average mixing ratios of the hourly concentration of ozone (O_3 in parts per billion by volume), nitric oxide (NO in parts per billion by volume), nitrogen dioxide (NO_2 in parts per billion by volume), nitrogen oxides (NO_x in parts per billion by volume), and total volatile organic compounds (TVOC in parts per billion by volume) in the stations of Viña del Mar (VM), Villa Alemana (VA), Quillota (QU), and Los Andes (LA) (average±standard deviation)

Pollutant (ppbv)	Sampling site			
	VM	VA	QU	LA
O_3	10.7±8.03	12.7±9.93	12.4±9.82	31.7±21.5
NO	15.4±15.2	8.75±14.6	3.86±5.33	2.29±4.12
NO_2	9.97±5.62	8.73±5.12	7.04±5.14	12.2±6.85
NO_x	25.4±18.0	17.5±17.0	10.9±8.58	14.5±9.46
TVOC	28.5±16.2	32.5±22.9	14.4±5.24	17.9±9.08

0.8 times than that observed in LA (14.5±9.46 ppbv) for VM, VA, and QU, respectively.

From the analysis of O_3 concentrations at ground level, it can be observed that the LA monitoring site exceeds the standard of air quality limit level of 61 ppbv average over an 8-h time span. However, in the VM, VA, and QU sites, the maximum O_3 levels have not exceed the O_3-8 h of 40-ppbv-concentration level. Generally, the 1-h average concentrations of O_3 are higher in the semi-urban areas (LA—31.7± 21.5 ppbv and QU—12.4±9.82 ppbv) and lower in the urban areas located near the coast (VM—10.7±8.03 ppbv and VA—12.7±9.93 ppbv). This observation can be explained by surface transport phenomena and/or by elevated ozone layer's
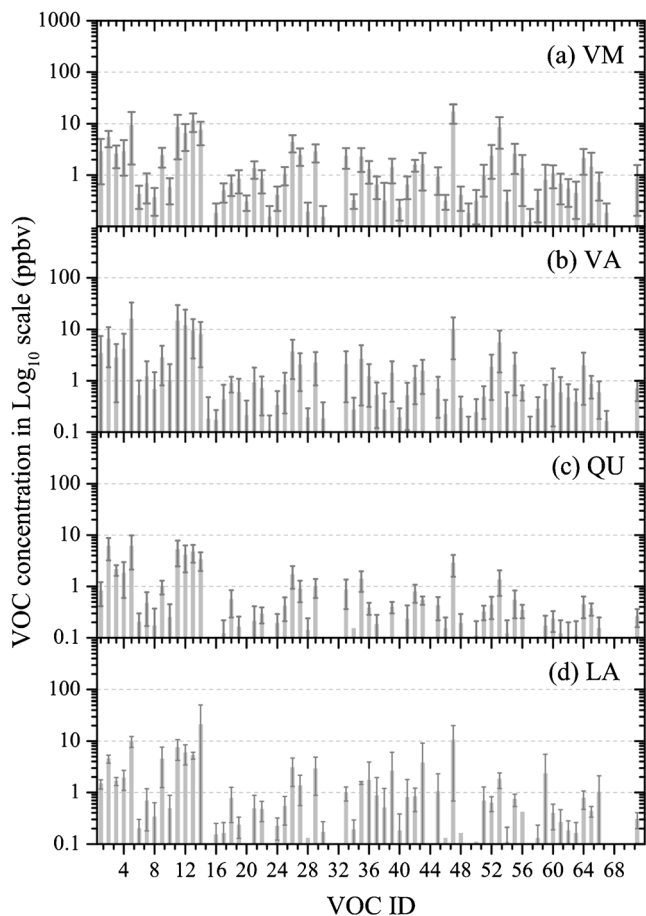

Fig. 4 The results of the ambient average concentrations with their respective standard deviations for each measured VOC in each of the sites under study in the sampling periods

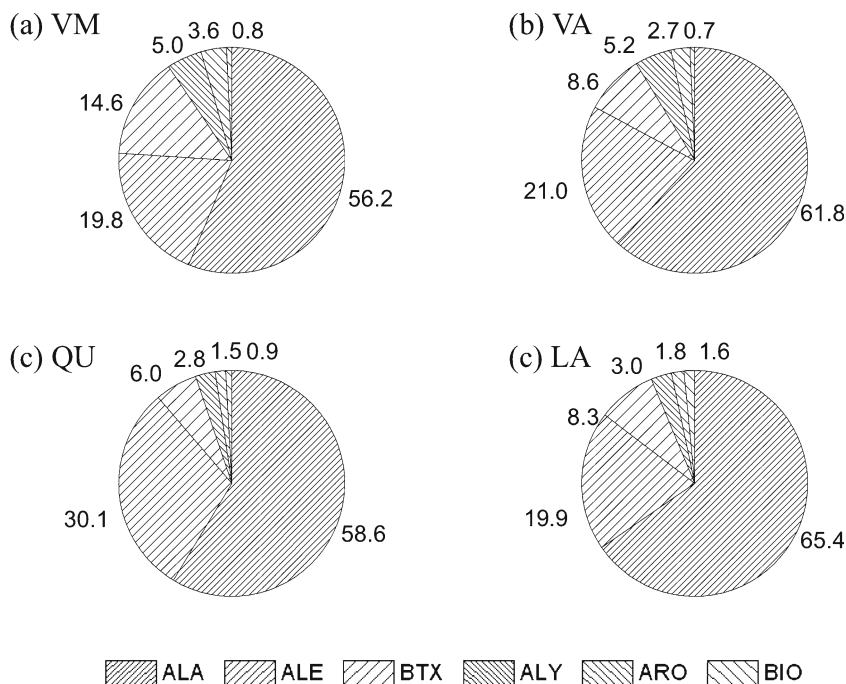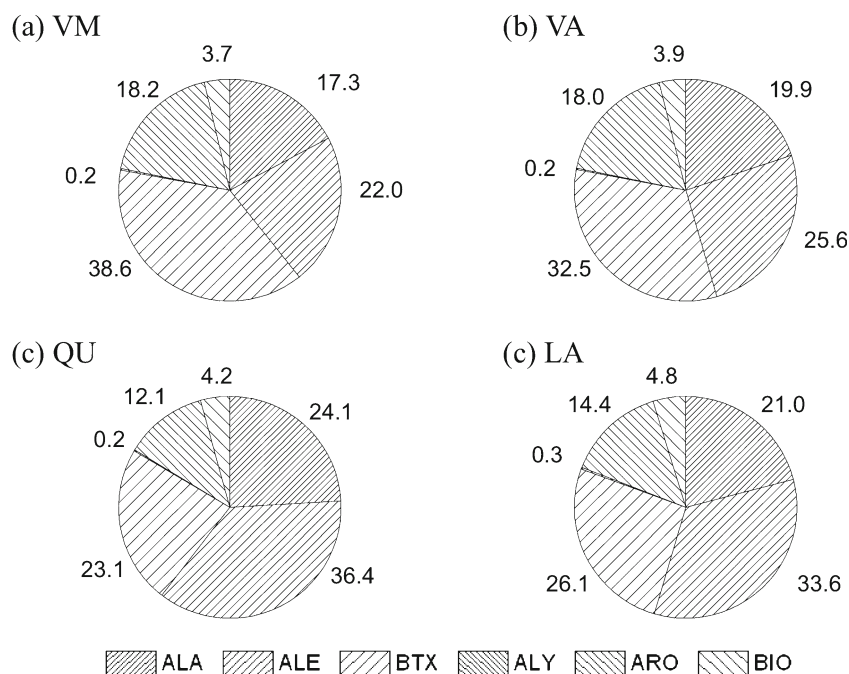**Fig. 3** The average contribution percentages for all of the analyzed samples of each VOC family

Fig. 5 The contribution percentages to the OFP by the VOC families (ALY, ALE, ALA, ARO, BTX, and BIO)

(a) VM

3.7
18.2
17.3
0.2
22.0
38.6

(b) VA

3.9
18.0
19.9
0.2
25.6
32.5

(c) QU

4.2
12.1
24.1
0.2
23.1
36.4

(c) LA

4.8
14.4
21.0
0.3
26.1
33.6

ALA ALE BTX ALY ARO BIO

contribution to local high-ozone episodes (Blumenthal et al. 1978; Seguel et al. 2013).

For the TVOC (71 VOC species, including alkanes, alkenes, and aromatic hydrocarbons), the higher concentrations were observed in VM and VA, which are approximately double that observed in QU and LA (see Table 3).

An analysis of variance was performed to establish the existence of significant differences in the concentrations of O_3 and NO_x between the sampling sites. The results, which are not shown here, indicate that, for both O_3 and NO_x, there are significant differences between the concentrations recorded at the different sampling sites.

VOC speciation

To analyze the species of VOCs, they were first grouped into different families of organic compounds, i.e., alkynes (ALI), alkenes (ALE), alkanes (ALA), aromatics (ARO), benzenes–toluene–xylenes (BTXs), and biogenics (BIO), from which the first families are mainly emitted by anthropogenic sources, while isoprene and alpha-pinene are mainly related to biogenic sources.

Figure 3 shows the average contribution percentages for all of the analyzed samples of each VOC family. These are in the range of 64–55 % for ALA, 30–19 % for ALE, 15–6 % for BTXs, 5.2–2.8 % for ALI, 3.6–1.5 % for ARO, and 1.5–0.7 % for BIO. Generally, the percentage contributions of the different VOC families are similar between the different sampling sites, with similar results found as for other sites reported in the literature (Chiang et al. 2007; Muezzinoglu et al. 2001; Na and Kim 2001; Zhang et al. 2008).

Figure 4 shows the results of the ambient average concentrations with their respective standard deviations for each
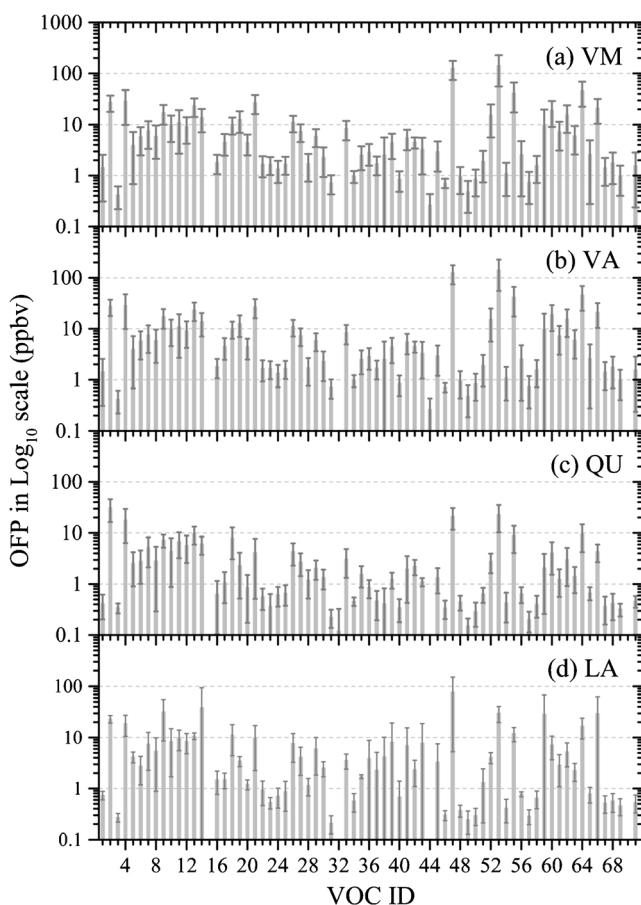

(a) VM

(b) VA

(c) QU

(d) LA

OFP in Log$_{10}$ scale (ppbv)

VOC ID

Fig. 6 Individual contribution of each VOC to the OFP

measured VOC in each of the sites under study in the sampling periods. First, Fig. 4 allows a comparison between the patterns of the organic species present in the studied sites to establish whether the contributions are similar. Generally, coincidence of the VOC atmospheric patterns is observed between the different studied sites. Second, it is possible to characterize the individual compounds that mostly contribute to the TVOC concentration. Hence, in the monitoring stations under study, the ten most abundant compounds in mass concentration are toluene (ID: 47), 2-methylpentane (ID: 26), pentane (ID: 14), 2-methylbutane (ID: 13), 2-methylpropane (ID: 12), butane (ID: 11), propane (ID: 5), and ethene (ID: 2). Also observed in the top ten compounds are propene (ID 4) in the case of the VM, VA, and QU sampling sites, m-, p-xylene (ID 53) at the VM and VA sampling sites, and, finally, ethane (ID: 3) and 2-methylpropene (ID: 9) at the QU and LA sampling sites, respectively.

Ozone photochemical sensitivity

The ozone photochemical sensitivity can be determined from an empirical approach based on the mean ambient mixing ratio of VOCs (in parts per billion carbon) and NO_x (in parts per billion by volume) (Geng et al. 2008; Jimenez and Baldasano 2004; Prabamroong et al. 2012; Sillman et al. 2003). An important stage in the development of effective strategies for ozone control is the evaluation of whether an area is limited by NO_x or limited by VOCs (Jimenez and Baldasano 2004; Prabamroong et al. 2012). To estimate the VOCs/NO_x mixing ratio, the concentrations recorded in the first hours of the morning are normally used. The results of the ratio between the concentrations of VOCs and NO_x (VOCs/NO_x, in parts per billion carbon/parts per billion by volume) show that the ratios for the VM, VA, QU, and LA sampling sites correspond to 1.12±0.1, 1.3±0.2, 0.7±0.1, and 0.9±0.1, respectively.

According to the VOCs/NO_x results, the sites under study are in an ozone formation regime that is VOC-limited. This implies that VOCs are sparse and NO_x is abundant. Therefore, the O_3 formation is insensitive to the change of NO_x levels and any slight changes of VOCs can significantly impact ozone formation (Kang et al. 2004; Martilli et al. 2002; Neftel et al. 2002). Consequently, when masses of air carrying a highly reactive mixture of VOCs and NO_x pass through areas with higher concentrations of VOC would experience severe ozone contamination.

Reactivity and ozone production by individual VOCs

In the present study, the reactivity of VOCs is evaluated by estimating the ozone formation potential (OFP). The procedure to calculate the OFP is described in several articles available in the literature (Carter 1994; Carter and Heo

2012; Zheng et al. 2009). The OFP is defined as, $OFP_i = MIR_i \times c_i$. Where OFP_i is calculated from the maximum incremental reactivity scale (MIR_i, listed in Carter and Heo 2012 and Table 2) and the ambient concentration for each VOC (c_i).

The total OFPs for the sites under study, arranged from highest to lowest, are 769, 668, 492, and 326 ppbv of O_3 production for VM, VA, LA, and QU, respectively. The total OFP/total VOCs mixing ratio, which indicates the reactivity of the VOC mixture with respect to the OFP capacity, presents the same tendency as that of the total OFP, that is, the VOC mixture is more reactive in VM with respect to LA, even when lower concentrations of ozone are observed in VM, which indicates that air masses with ozone are being transported to LA.

Figure 5 shows the contribution percentages to the OFP by the VOC families (ALY, ALE, ALA, ARO, BTX, and BIO). It can be observed that, in terms of the OFP, the VOC families with higher contributions are BTX, ALE, ALA, and ARO, with values in the ranges of 38.6–23.1, 36.4–22.0, 24.1–17.3, and 18.2–12.1 %, respectively. It can be observed that, for the BTX and ALA families, the higher contributions are found in VM, followed by VA, QU, and finally, LA. In contrast, in the case of ALE and ALA, the higher contributions are seen at the LA and QU sites, while the lowest contributions are seen at VM and VA. Finally, the contributions of the BIO and ALY families are the lowest, with values in the ranges of 4.76–3.70 and 0.25–0.17 %, respectively.

There is a significant difference when calculating the OFP contribution percentages of each family using the mass concentration with respect to the contribution calculated considering the reactivity. In the calculation that incorporates the mass concentration, the contribution in decreasing order is ALA > ALE > BTX > ALY > ARO > BIO; however, when considering the reactivity, the order is BTX > ALE > ALA > ARO > BIO > ALY. This difference indicates that more effective management measures to reduce contamination due

Table 4 The m-, p-xylene/ethylbenzene ratios (mpX/EB) obtained from the linear regression analysis (correlation coefficient R^2) of the data obtained in the morning hours (0600–1000 hours LT) and in the afternoon (1200–1600 hours) at the monitoring sites of Viña del Mar (VM), Villa Alemana (VA), Quillota (QU), and Los Andes (LA)

Sampling site	Sampling time (LT)	Ratio mpX/EB	Correlation coef. (R^2)
VM	0600–1000	0.286±0.004	0.998
	1200–1600	0.276±0.003	0.999
VA	0600–10:00	0.320±0.018	0.986
	1200–1600	0.350±0.016	0.988
LA	0600–1000	0.319±0.003	0.999
	1200–1600	0.428±0.013	0.995

to ozone photochemical reactions must consider the VOC activities, suggesting that the efforts should be focused on families or specific compounds.

Figure 6 shows the individual contribution of each VOC to the OFP. Generally, similar behaviors are observed at all of the studied sites. In the urbanized sites, such as VM and VA, the higher contributions are given by m-, p-xylene (ID 53), o-xylene (ID 55), toluene (ID 47), propene (ID 4), and ethene (ID 5), all of which are chemical compounds emitted from anthropogenic sources with the potential to contribute significantly to the formation of ozone. In the LA location, which is characterized as a semi-urban site with high agricultural activity in its surroundings, it is found that alpha-pinene (ID 59) is among the VOCs with higher contributions to the OFP, which indicates that the environment surrounding the LA site would be impacted by biogenic emissions. Generally, these species have long atmospheric lifetimes, allowing them to be transported toward areas that receive wind; as a result, the areas receiving air masses enriched with VOCs are significantly impacted in terms of ozone formation.

Transport and photochemical aging

The m-, p-xylene/ethylbenzene ratio has been widely used to identify the degree of evolution of the photochemical reactions of the air masses that are transported to a determined area, also known as the air mass "age" (Zhang et al. 2008; Nelson and Quigley 1983; Shiu et al. 2007; Shao et al. 2011; Wang et al. 2008). With a high photochemical activity, the p-xylene/ethylbenzene ratio becomes higher because the gas phase m-, p-xylene has a reaction constant with OH, at 298 K and 1 atm (m-xylene, $kOH = 23.6 \times 10^{-12}$ cm^3 molecule^{-1} s^{-1}; p-xylene, $kOH = 14.3 \times 10^{-12}$ cm^3 molecule^{-1} s^{-1}) that is larger in comparison to that of ethylbenzene (7.1×10^{-12} cm^3 molecule^{-1} s^{-1}) (Seguel et al. 2013).

Table 4 presents the values of the m-, p-xylene/ethylbenzene ratio from the linear regression analysis of the available values for the morning hours (0600–1000 hours LT) and the afternoon (1200–1600 hours LT), that is, the time of higher photochemical activity. At the QU monitoring station, it was not possible to obtain a relation from the linear regression analysis due to the limited number of data. The results indicate that the ethylbenzene and m-, p-xylene ambient concentrations at the different sampling sites present a high correlation, with correlation coefficients (R^2) in the range of 0.986 to 0.999 for the three sites (VM, VA, and LA). The latter result implies that these compounds are emitted from the same source, i.e., vehicle emissions. Moreover, it can be observed that the relationship increases from VM to LA during the afternoon (1200–1600 hours). The results indicate that aged air masses arrive in the LA area. Furthermore, in the morning, the relationships are practically the same in the different study

sites, which indicates that the morning is the period of the maximum emissions of these compounds, associated with the increased flow of vehicles in the morning.

Finally, the values of mpX/EB in the sites under study are similar to those observed in other cities around the world, such as Guangzhou in China (0.21) (Wang et al. 2003), Izmir in Turkey (0.45) (Muezzinoglu et al. 2001), and Seoul in Korea (0.30) (Na and Kim 2001).

Conclusions

An intensive measurement campaign was conducted during the summer of 2010 at four sites located in the area of the V Region of Valparaiso in Chile. Measurements of O$_3$, NO, NO$_x$, and 71 VOCs were performed to characterize their compositions and concentration distributions, to illustrate the general characteristics of the different types of VOCs, and to evaluate the OFPs and the ages of air parcels using relational data techniques.

Higher ozone concentrations were observed in the windward sites (LA) relative to the leeward sites (VM) due to the different stages of the photochemical reaction. The VM and VA sites present higher concentrations of NO$_x$ and VOCs precursors. The organic species patterns show a high coincidence in the studied localities, mainly between the VA, QU and LA sites. An environmental pattern characteristic of a composition corresponding to vehicle emissions was observed.

The OFP estimation is a better indicator than the VOC mass concentration in order to evaluate the contribution to ozone formation because these take into consideration of the reactivity of each VOC. The results indicate that ethene, propene, toluene, and xylenes are the organic species with higher contributions to ozone for the sites studied under a VOC-limited regime.

The results of m-p-xylene/ethylbenzene ratio provide evidence of the receptor condition of the aged air masses at the LA site. However, the result does not provide evidence of the origin of these masses of air, thereby requiring atmospheric modeling studies.

The results presented in this study reveal that ozone pollution is a regional problem and that the LA area, which presently lacks ozone pollution surveillance measures, is affected by elevated levels of ozone that are not locally produced. In this way, the results relevant to the obtained data are representative of the O$_3$ precursors, especially the VOCs, in an area under constant development, showing the first signs of air quality deterioration as a result of photochemical contamination.

References

Adame JA, Sole JG (2013) Surface ozone variations at a rural area in the northeast of the Iberian Peninsula. Atmos Pollut Res 4:130–141

Avery RJ (2006) Reactivity-based VOC control for solvent products: more efficient ozone reduction strategies. Environ Sci Technol 40: 4845–4850

Blumenthal DL, White WH, Smith TB (1978) Anatomy of a Los Angeles smog episode: pollutant transport in the daytime sea breeze regime. Atmos Environ 12:893–907

Camredon M, Aumont B, Lee-Taylor J, Madronich S (2007) The SOA/VOC/NO_x system: an explicit model of secondary organic aerosol formation. Atmos Chem Phys 7:5599–5610

Carter WPL (1994) Development of ozone reactivity scales for volatile organic-compounds. J Air Waste Manage 44:881–899

Carter WPL, Heo G (2012) Development of revised SPARC aromatics mechanisms. Final Report to California Air Resources Board Contracts No. 07-730 and 08-326

Chiang HL, Tsai JH, Chen SY, Lin KH, Ma SY (2007) VOC concentration profiles in an ozone non-attainment area: a case study in an urban and industrial complex metroplex in southern Taiwan. Atmos Environ 41:1848–1860

Denisov ET (2008) Mechanisms of the reactions of radicals with ozone. Russ J Phys Chem B 2:58–66

DMG (2013) Climatología. Dirección Meteorológica de Chile, Dirección General de Aeronáutica Civil, Santiago, Chile. http://www.meteochile.gob.cl. Accessed Oct 2013

Fenger J (2009) Air pollution in the last 50 years—from local to global. Atmos Environ 43:13–22

Geng FH, Tie XX, Xu JM, Zhou GQ, Peng L, Gao W, Tang X, Zhao CS (2008) Characterizations of ozone, NO_x, and VOCs measured in Shanghai, China. Atmos Environ 42:6873–6883

IGM (2013) Cartografía. Instituto Geográfico Militar. http://www.igm.cl

INE (2013) Statistical Products. Instituto Nacional de Estadísticas, Chile. http://www.ine.cl. Accessed Oct 2013

Jacob D (1999) Introduction to atmospheric chemistry. Princeton University Press, Princeton

Jimenez P, Baldasano JM (2004) Ozone response to precursor controls in very complex terrains: use of photochemical indicators to assess O_3-NO_x-VOC sensitivity in the northeastern Iberian Peninsula. J Geophys Res-Atmos 109

Kang DW, Aneja VP, Mathur R, Ray JD (2004) Observed and modeled VOC chemistry under high VOC/NO_x conditions in the Southeast United States national parks. Atmos Environ 38:4969–4974

Martilli A, Neftel A, Favaro G, Kirchner F, Sillman S, Clappier A (2002) Simulation of the ozone formation in the northern part of the Po Valley. J Geophys Res-Atmos 107

MMA (2011) Official Environment Status Report 2011. Ministerio del Medio Ambiente, Chile. http://www.mma.gob.cl/1304/w3-article-52016.html. Accessed Oct 2013

Morales RGE (2006) Atmospheric urban pollution. Critical episodes of the environmental pollution in the City of Santiago of Chile (in Spanish). Editorial Universitaria SA, Santiago of Chile. ISBN 956-11-1835-1, 324 pp

Muezzinoglu A, Odabasi M, Onat L (2001) Volatile organic compounds in the air of Izmir, Turkey. Atmos Environ 35:753–760

Na K, Kim YP (2001) Seasonal characteristics of ambient volatile organic compounds in Seoul, Korea. Atmos Environ 35:2603–2614

Neftel A, Spirig C, Prevot ASH, Furger M, Stutz J, Vogel B, Hjorth J (2002) Sensitivity of photooxidant production in the Milan Basin: an overview of results from a EUROTRAC-2 Limitation of Oxidant Production field experiment. J Geophys Res-Atmos 107

Nelson PF, Quigley SM (1983) The m, p-xylenes:ethylbenzene ratio. A technique for estimating hydrocarbon age in ambient atmospheres. Atmos Environ 17:659–662

Prabamroong T, Manomaiphiboon K, Limpaseni W, Sukhapan J, Bonnet S (2012) Ozone and its potential control strategy for Chon Buri City, Thailand. J Air Waste Manage 62:1411–1422

Pusede SE, Cohen RC (2012) On the observed response of ozone to NO_x and VOC reactivity reductions in San Joaquin Valley California 1995–present. Atmos Chem Phys 12:8323–8339

Sawyer RF (2010) Vehicle emissions: progress and challenges. J Expo Sci Environ Epidemiol 20:487–488

Seguel RJ, Morales RGE, Leiva MA (2012) Ozone weekend effect in Santiago, Chile. Environ Pollut 162:72–79

Seguel RJ, Mancilla CA, Rondanelli R, Leiva MA, Morales RGE (2013) Ozone distribution in the lower troposphere over complex terrain in Central Chile. J Geophys Res-Atmos 118:2966–2980

Seinfeld JH, Pandis SN (2012) Atmospheric chemistry and physics: from air pollution to climate change. Wiley, New York

Shao M, Wang B, Lu S, Yuan B, Wang M (2011) Effects of Beijing Olympics control measures on reducing reactive hydrocarbon species. Environ Sci Technol 45:514–519. doi:10.1021/es102357t

Shiu C-J, Liu SC, Chang C-C, Chen J-P, Chou CCK, Lin C-Y, Young C-Y (2007) Photochemical production of ozone and control strategy for Southern Taiwan. Atmos Environ 41:9324–9340

Sillman S, Vautard R, Menut L, Kley D (2003) O_3-NO_x-VOC sensitivity and NO_x-VOC indicators in Paris: results from models and atmospheric pollution over the Paris area (ESQUIF) measurements. J Geophys Res-Atmos 108

SINCA (2013) Sistema Nacional de Calidad del Aire. Ministerio de Medio Ambiente, Chile. http://www.mma.gob.cl/1304/w3-article-52016.html. Accessed Oct 2013

US-EPA (1999a) Compendium Method TO-14A: determination of volatile organic compounds (VOCs) in ambient air using specially prepared canisters with subsequent analysis by gas chromatography. compendium of methods for the determination of toxic organic compounds in ambient air, Second Edition, Center for Environmental Research Information Office of Research and Development, U.S. Environmental Protection Agency, Cincinnati, OH, USA. http://www.epa.gov/ttnamti1/files/ambient/airtox/to-14ar.pdf. Accessed Oct 2013

US-EPA (1999b) Compendium Method TO-15: determination of volatile organic compounds (VOCs) in air collected in specially-prepared canisters and analyzed by gas chromatography/mass spectrometry (GC/MS). Compendium of methods for the determination of toxic

organic compounds in ambient air, Second Edition, Center for Environmental Research Information Office of Research and Development, U.S. Environmental Protection Agency, Cincinnati, OH, USA. http://www.epa.gov/ttnamti1/files/ambient/airtox/to-14ar.pdf. Accessed Oct 2013

Vivanco MG (2008) Relation between ozone levels and NO_x and VOC emissions in the Sao Paulo Metropolitan Area for an episode of August, 1998. Int J Environ Pollut 35:90–98

Wang ZH, Zhang SY, Lu SH, Bai YH (2003) Screenings of 23 plant species in Beijing for volatile organic compound emissions. Chin J Environ Sci 24:7–12

Wang JL, Wang CH, Lai CH, Chang CC, Liu Y, Zhang YH, Liu S, Shao M (2008) Characterization of ozone precursors in the Pearl River Delta by time series observation of nonmethane hydrocarbons. Atmos Environ 42:6233–6246

Zhang HL, Ying Q (2011) Contributions of local and regional sources of NO_x to ozone concentrations in Southeast Texas. Atmos Environ 45:2877–2887

Zhang J, Wang T, Chameides WL, Cardelino C, Blake DR, Streets DG (2008) Source characteristics of volatile organic compounds during high ozone episodes in Hong Kong, Southern China. Atmos Chem Phys 8:4983–4996

Zheng JY, Shao M, Che WW, Zhang LJ, Zhong LJ, Zhang YH, Streets D (2009) Speciated VOC emission inventory and spatial patterns of ozone formation potential in the Pearl River Delta, China. Environ Sci Technol 43:8580–8586